ISSN 2176-5480

22nd International Congress of Mechanical Engineering (COBEM 2013)
November 3-7, 2013, Ribeirão Preto, SP, Brazil

NONLINEAR ATTITUDE CONTROL OF ARTIFICIAL SATELLITES CONSIDERING FAILURE IN MOMENTUM WHEELS

Carlos Augusto de Carvalho Junior
Universidade Federal do ABC / Aerospace Engineering
Av. dos Estados, 5001 - Bangu - Santo André
carlos.carvalho@ufabc.edu.br

Andre Fenili
Universidade Federal do ABC / Aerospace Engineering
Av. dos Estados, 5001 - Bangu - Santo André
andre.fenili@ufabc.edu.br

Abstract. *This paper develops theoretical and numerical analysis regarding a problem that occurs in artificial satellites: mechanical failure in the momentum wheels. The artificial satellite to be investigated consists of a rigid body freely to move around the three axes. In each one of these directions a momentum wheel is placed in order to control the attitude angle around that axes. A linear control law or a nonlinear control law can be applied on each one of the momentum wheels. The linear control technique studied here is the Linear Quadratic Regulator (LQR) and the non-linear technique is the State Dependent Riccati Equation (SDRE). The mathematical model with the different control laws is numerically integrated using the fourth order Runge-Kutta. The cases tested in this paper take into consideration failures in one or in two of the three momentum wheels and the ability of each one of the proposed controllers to satisfactorily control the satellite under these conditions.*

Keywords: *artificial satellites, attitude control, momentum wheels, LQR, nonlinear control, SDRE.*

1. INTRODUCTION

A meteorological satellite must be appointed to some region of the planet Earth in order to acquisite images which are subsequently used for weather forecasting. This acquisition must be precise and stable to disturbances to ensure useful images. The pointing of the acquisition camera and the robustness of this appointment are provided by means of actuation devices called momentum wheels (or reaction wheels, in some cases).

Reaction/momentum wheels are flywheels used to provide attitude control authority and stability on spacecraft. By adding or removing energy from the flywheel, torque is applied to a single axis of the spacecraft, causing it to react by rotating. By maintaining flywheel rotation, called momentum, a single axis of the spacecraft is stabilized. Several reaction/momentum wheels can be used to provide full three-axis attitude control and stability

In general, each one of the principal axes of the satellite is controlled by one momentum wheel. In some cases, a fourth momentum wheel is positioned strategically for the situation in which one of those three presents some failure. The additional wheel must surpass the deficiency and ensure the continued operation of the satellite (Agrawal, 1986; Fenili e Kuga, 2008).

Three momentum wheels are considered here. Each one of these wheels is aligned with a principal axes of the satellite. Two cases are considered in this paper: (1) each one of the momentum wheels is controlled by a linear control law named LQR (Dorato et al., 1995) and (2) each one of the momentum wheels is controlled by a nonlinear control law named SDRE (Çimen, 2008). These two cases are compared when one or two of the wheels just stop working during an operation.

2. THE GOVERNING EQUATIONS OF MOTION

The angular momentum of a rigid body with respect to its center of mass is given by:

$$\vec{H} = J\,\vec{\omega} \tag{1}$$

with H being the body´s angular momentum, J being the inertia tensor and ω being the angular velocity of the body relative to the inertial frame.

The rate of change of $\vec{H}$ equals the total external torque acting on the body. In the special case when the body axes x, y and z are the principal axes of inertia, let $\bar{I}_x$, $\bar{I}_y$ and $\bar{I}_z$ be the principal moments of inertia.

In this situation, the governing equations of motion given by Eq. (1) can be expanded as:

ISSN 2176-5480

$$\begin{aligned}\sum M_x &= \bar{I}_x\dot{\omega}_x - \left(\bar{I}_y - \bar{I}_z\right)\omega_z\omega_y \\ \sum M_y &= \bar{I}_y\dot{\omega}_y - \left(\bar{I}_z - \bar{I}_x\right)\omega_z\omega_x \\ \sum M_z &= \bar{I}_z\dot{\omega}_z - \left(\bar{I}_x - \bar{I}_y\right)\omega_x\omega_y\end{aligned} \tag{2}$$

Equations (2) are called the Euler's equations of motion.

The shape of the satellite considered in this paper sis a cube. For the cube one has $\bar{I}_x = \bar{I}_y = \bar{I}_z = \bar{I}$. Using this simplification in Eq. (2) and considering only one external torque acting in each direction, the following set of governing equations is obtained:

$$\begin{aligned}M_x &= \bar{I}_x\dot{\omega}_x \\ M_y &= \bar{I}_y\dot{\omega}_y \\ M_z &= \bar{I}_z\dot{\omega}_z\end{aligned} \tag{3}$$

The relationship between the angular velocity ω in each direction and the Euler´s angles used in this work is given by:

$$\begin{aligned}\omega_x &= \dot{\phi}\cdot\sin\theta\cdot\sin\psi + \dot{\theta}\cdot\cos\psi \\ \omega_y &= \dot{\phi}\cdot\sin\theta\cdot\cos\psi + \dot{\theta}\cdot\sin\psi \\ \omega_z &= \dot{\phi}\cdot\cos\theta + \dot{\psi}\end{aligned}$$

Using this relationship in Eq. (3) results:

$$\begin{aligned}&\ddot{\varphi}\sin\theta\sin\psi + \ddot{\theta}\cos\psi + \dot{\varphi}\dot{\theta}\cos\theta\sin\psi + \dot{\varphi}\dot{\psi}\sin\theta\cos\psi - \dot{\theta}\dot{\psi}\sin\psi = \frac{M_x}{\bar{I}_x} \\ &\ddot{\varphi}\sin\theta\cos\psi - \ddot{\theta}\sin\psi + \dot{\varphi}\dot{\theta}\cos\theta\cos\psi + \dot{\varphi}\dot{\psi}\sin\theta\sin\psi - \dot{\theta}\dot{\psi}\cos\psi = \frac{M_y}{\bar{I}_y} \\ &\ddot{\psi} + \ddot{\varphi}\cos\theta - \dot{\varphi}\dot{\theta}\sin\theta = \frac{M_z}{\bar{I}_z}\end{aligned} \tag{4}$$

Decoupling the second derivatives, it is possible to write the governing equations of motion for the problem investigated here as:

$$\begin{aligned}\ddot{\theta} &= \frac{M_x\sin\psi}{I} + \frac{M_y\sin\psi}{I} - \dot{\phi}\dot{\theta}\,\mathrm{sen}\,\theta \\ \ddot{\phi} &= \frac{1}{\sin\theta}\left(\frac{M_x\sin\psi}{I} + \frac{M_y\sin\psi}{I} - \dot{\phi}\dot{\theta}\cos\theta + \dot{\psi}\dot{\theta}\right) \\ \ddot{\psi} &= \frac{M_z}{I} - \frac{\cos\theta}{\sin\theta}\left(\frac{M_x\sin\psi}{I} + \frac{M_y\sin\psi}{I} - \dot{\phi}\dot{\theta}\cos\theta + \dot{\psi}\dot{\theta}\right) + \dot{\phi}\dot{\theta}\,\mathrm{sen}\,\theta\end{aligned} \tag{5}$$

3. LINEAR AND NONLINEAR CONTROL

3.1 The Linear Quadratic Regulator (LQR)

The LQR-strategy is based on defining a cost function which shall be minimized. By doing this one can obtain a gain matrix of optimal gains to be used for feedback. In this paper, one considers a quadratic cost function given by:

$$J = \int_0^\infty L(x^T Q x + u^T R u)\,dt \tag{6}$$

ISSN 2176-5480

And the steady-state LQR problem. The optimum linear control law that minimizes the quadratic cost function J assumed here is given, according to (Dorato et al., 1995), by:

$$U = -R^{-1}B^{T}Kx \tag{7}$$

In Eq. (7), K is a symmetric positive definite matrix that satisfies the matrix Algebraic Ricatti Equation given by:

$$A^{T}K + KA + Q - KBR^{-1}B^{T}K = 0 \tag{8}$$

Equation (8), Q and R are positive definite weighting matrices.

The linear system matrices A and B used for the determination of the optimal gains is obtained by neglecting all the nonlinear terms.

3.2 The State-dependent Riccati equation (SDRE)

The state-dependent Riccati equation (SDRE) approach to nonlinear system control relies on representing a nonlinear system's dynamics with state-dependent coefficient matrices that can be inserted into state-dependent Riccati equations to generate a feedback law (Shamma and Cloutier, 2003). The main idea of this method is to represent the nonlinear system:

$$\dot{x} = f(x) + B(x)u \tag{9}$$

In the form:

$$\dot{x} = A(x)\,x + B(x)u \tag{10}$$

The feedback law is given by (Shamma and Cloutier, 2003):

$$u = -R^{-1}(x)\;B^{T}(x)\;P(x)\;x \tag{11}$$

Where P(x) is obtained from the SDRE:

$$P(x)A(x) + A^{T}(x)P(x) + Q(x) - P(x)B(x)R^{-1}(x)B^{T}(x)P(x) = 0 \tag{12}$$

In Eq. 12, Q(x) and R(x) are design parameters that satisfy the positive definiteness condition $Q(x) > 0$ and $R(x) > 0$.

3.3 Linearization technique

For nonlinear systems sometimes it is important to verify the dynamics near the equilibrium points. An analysis that can be conducted is the linearization around this point. The stability of the original system around this point is related to the behaviour of the linear system that approximates it around this point. Let an autonomous system ne given by:

$$\begin{cases} \dfrac{dy}{dx} = f(x,y) \\ \dfrac{dy}{dx} = g(x,y) \end{cases}$$

With the equilibrium point (x_0,y_0). The linearization is obtained near this point using an expansion in Taylor series given by:

ISSN 2176-5480

$$f(x,y) \approx f(x_0,y_0) + \left.\frac{df}{dx}\right|_{(x_0,y_0)} (x-x_0) + \left.\frac{df}{dy}\right|_{(x_0,y_0)} (y-y_0)$$

$$g(x,y) \approx g(x_0,y_0) + \left.\frac{dg}{dx}\right|_{(x_0,y_0)} (x-x_0) + \left.\frac{dg}{dy}\right|_{(x_0,y_0)} (y-y_0)$$

The resulting linear system has coefficient matrix

$$\begin{bmatrix} \left.\frac{df}{dx}\right|_{(x_0,y_0)} & \left.\frac{df}{dy}\right|_{(x_0,y_0)} \\ \left.\frac{dg}{dx}\right|_{(x_0,y_0)} & \left.\frac{dg}{dy}\right|_{(x_0,y_0)} \end{bmatrix} \tag{13}$$

4. LINEARIZATION OF THE GOVERNING EQUATIOINS OF MOTION

To apply the LQR one needs first to linearize the governing equations of motion, since the LQR works with linear systems. The states considered here are:

$$\begin{aligned} x_1 &= \theta \\ x_2 &= \dot{\theta} \\ x_3 &= \phi \\ x_4 &= \dot{\phi} \\ x_5 &= \psi \\ x_6 &= \dot{\psi} \end{aligned} \tag{14}$$

The linearization of Eq. (5) using the linearization technique discussed in Sub-Chapter 3.3 is realized in the neighbourhood of the states:

$$\begin{aligned} x_1 &= \frac{\pi}{2} \\ x_2 &= 0 \\ x_3 &= 0 \\ x_4 &= 0 \\ x_5 &= 0 \\ x_6 &= 0 \end{aligned} \tag{15}$$

The linearized governing equations of motion are then given by:

$$\begin{Bmatrix} \dot{x}_1 \\ \dot{x}_2 \\ \dot{x}_3 \\ \dot{x}_4 \\ \dot{x}_5 \\ \dot{x}_6 \end{Bmatrix} = \begin{bmatrix} 0 & 1 & 0 & 0 & 0 & 0 \\ 0 & 0 & 0 & 0 & 0 & 0 \\ 0 & 0 & 0 & 1 & 0 & 0 \\ 0 & 0 & 0 & 0 & 0 & 0 \\ 0 & 0 & 0 & 0 & 0 & 1 \\ 0 & 0 & 0 & 0 & 0 & 0 \end{bmatrix} \begin{Bmatrix} x_1 - \frac{\pi}{2} \\ x_2 \\ x_3 \\ x_4 \\ x_5 \\ x_6 \end{Bmatrix} + \begin{bmatrix} 0 & 0 & 0 & 0 & 0 & 0 \\ 0 & \frac{1}{I} & 0 & -\frac{1}{I} & 0 & 0 \\ 0 & 0 & 0 & 0 & 0 & 0 \\ 0 & 0 & 0 & \frac{1}{I} & 0 & 0 \\ 0 & 0 & 0 & 0 & 0 & 0 \\ 0 & 0 & 0 & 0 & 0 & \frac{1}{I} \end{bmatrix} \begin{Bmatrix} 0 \\ M_x \\ 0 \\ M_y \\ 0 \\ M_z \end{Bmatrix} \tag{16}$$

ISSN 2176-5480

5. STATE DEPENDENT MATRICES FOR THE SDRE

The implementation of the SDRE uses the original governing equations of motion given by Eq. (5) but in the state space form. These equations when written in the form given by Eq. (10) have the A and B matrices as state dependent quantities given by:

$$A(x)=\begin{vmatrix} 0 & 1 & 0 & 0 & 0 & 0 \\ 0 & 0 & 0 & -x_2\sin(x_1) & 0 & 0 \\ 0 & 0 & 0 & 1 & 0 & 0 \\ 0 & 0 & 0 & -x_2\cos(x_1)/\sin(x_1) & 0 & x_2/\sin(x_1) \\ 0 & 0 & 0 & 0 & 0 & 1 \\ 0 & -x_6\cos(x_1)/\sin(x_1) & 0 & x_4\cos(x_1)/\sin(x_1) & 0 & x_2/\sin(x_1) \end{vmatrix} \tag{17}$$

And:

$$B(x)=\begin{vmatrix} 0 & 0 & 0 & 0 & 0 & 0 \\ 0 & \cos(x_5)/I & 0 & -\sin(x_5)/I & 0 & 0 \\ 0 & 0 & 0 & 0 & 0 & 0 \\ 0 & \sin(x_5)/(I\sin(x_1)) & 0 & \cos(x_5)/(I\sin(x_1)) & 0 & 0 \\ 0 & 0 & 0 & 0 & 0 & 0 \\ 0 & -\sin(x_5)\cos(x_1)/(I\sin(x_1)) & 0 & -\cos(x_5)\cos(x_1)/(I\sin(x_1)) & 0 & 1/I \end{vmatrix} \tag{18}$$

Matrix A can be written in several ways. The form presented in Eq. (17) is just one of them. In this sense, one deals here with a sub-optimal problem.

6. NUMERICAL SIMULATIONS

The parameters and initial conditions used in the numerical simulations are presented in Tab. 1 and 2.

Table 1. Parameters used in the numerical simulations

Parameter	Value
acceleration of gravity	9.81m/s^2
total time	200 s
integration step	10^{-2}
total mass fo the satellite	200 Kg
dimension of the cube (satellite)	0.6m

Table 2. Initial conditions for the angular positions and angular velocities

Initial conditions	Value
$\theta(0)$	0.8 rad
$\phi(0)$	0.7 rad
$\Psi(0)$	0.6 rad
$\dot{\theta}(0)$	0.04 rad/s
$\dot{\phi}(0)$	0.04 rad/s
$\dot{\psi}(0)$	0.04 rad/s

The weighting matrices Q and R considered in the numerical simulations are:

ISSN 2176-5480

$$Q = \begin{bmatrix} 50 & 0 & 0 & 0 & 0 & 0 \\ 0 & 50 & 0 & 0 & 0 & 0 \\ 0 & 0 & 10 & 0 & 0 & 0 \\ 0 & 0 & 0 & 10 & 0 & 0 \\ 0 & 0 & 0 & 0 & 10 & 0 \\ 0 & 0 & 0 & 0 & 0 & 10 \end{bmatrix} \tag{19}$$

And

$$R = \begin{bmatrix} 50 & 0 & 0 & 0 & 0 & 0 \\ 0 & 50 & 0 & 0 & 0 & 0 \\ 0 & 0 & 100 & 0 & 0 & 0 \\ 0 & 0 & 0 & 100 & 0 & 0 \\ 0 & 0 & 0 & 0 & 100 & 0 \\ 0 & 0 & 0 & 0 & 0 & 100 \end{bmatrix} \tag{20}$$

6.1 Failure of the momentum wheel considering the LQR

The failure of the momentum wheel is considered in the numerical simulations by imposing that the torques M_x, M_y or M_z are zero after some integration time. It means that the specific wheel is not actuating anymore. Only LQR control is considered here.

First one considers that M_x (the torque associated to the angle θ) fails. It occurs after 15 seconds of operation. The results are presented in Fig. 1 and 2.

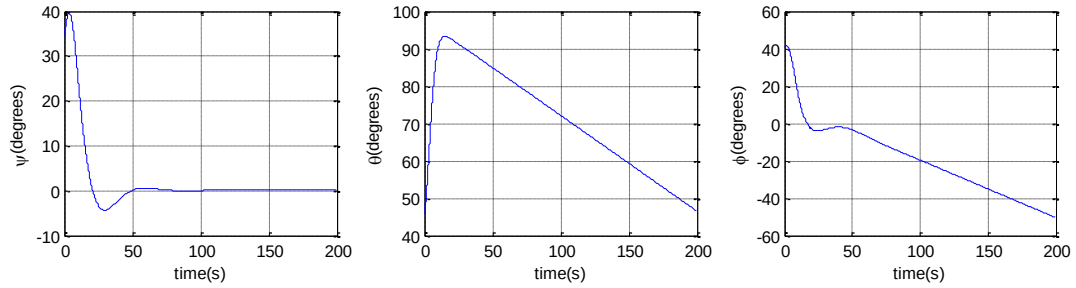

Figure 1. Attitude angles θ, Ψ and ϕ with failure in M_x after 15s: LQR control.

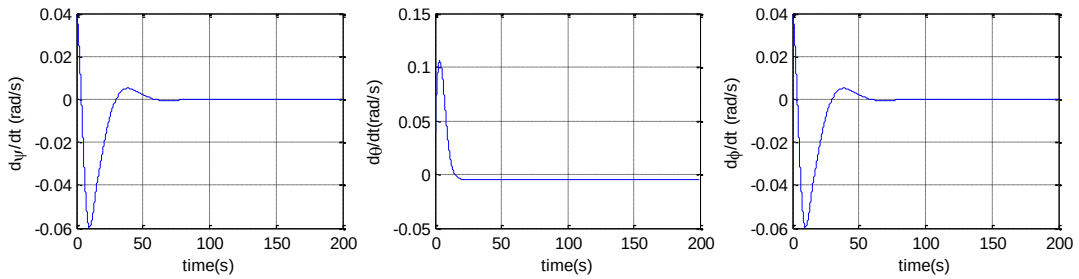

Figure 2. Angular velocity dθ/dt, dΨ/dt and dϕ/dt with the failure in M_x after 15s: LQR control.

It is observed that with the failure of the torque M_x the velocity $\dot{\theta}$ do not converges to zero. It causes instability in this angle and in the angle ϕ. The torques M_y and M_z brings the angles ϕ and Ψ to zero.

One considers now that M_y (the torque associated to the angle ϕ) fails. The results are presented in Fig. 3 and 4.

ISSN 2176-5480

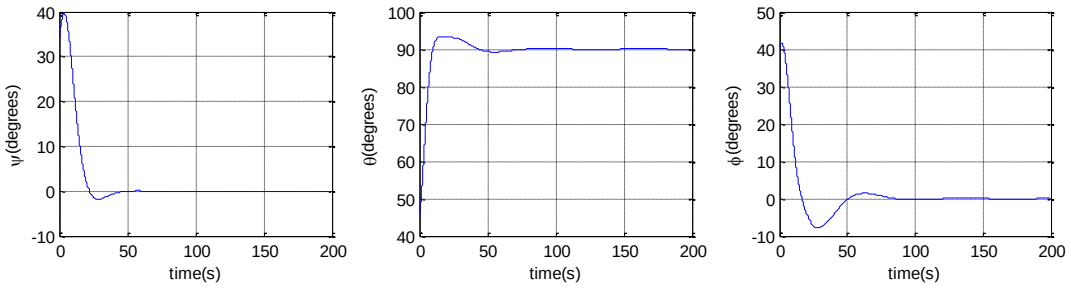

Figure 3. Attitude angles θ, Ψ and ϕ with failure in M_y after 15s: LQR control.

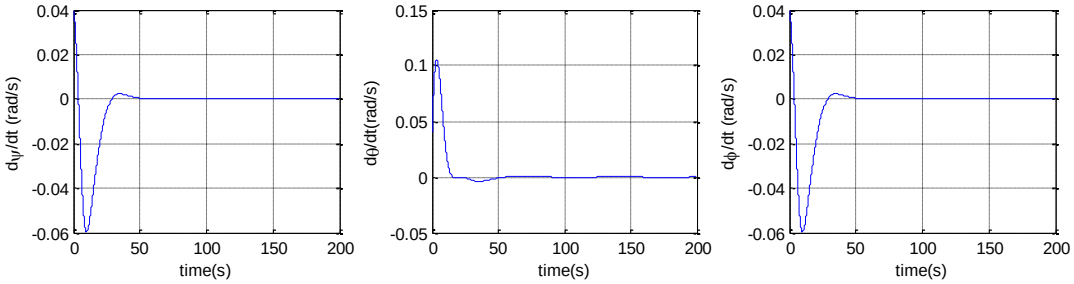

Figure 4. Angular velocity dθ/dt, dΨ/dt and dϕ/dt with the failure in M_y after 15s: LQR control.

Even with the failure in M_y it can be noted that the system is stable in the other two directions during the period of the simulation. This occurs because the coupling between θ, Ψ and ϕ. The dynamics and control in the angles θ and Ψ are able to compensate the failure in the momentum wheel acting on ϕ.

One considers now that M_z (the torque associated to the angle Ψ) fails. The results are presented in Fig. 5 and 6.

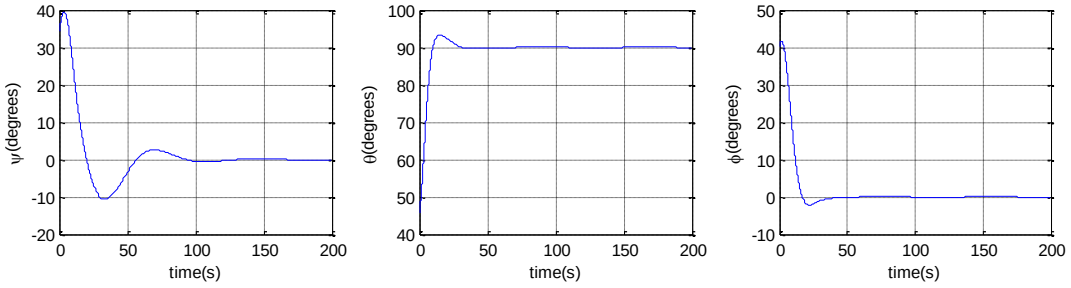

Figure 5. Attitude angles θ, Ψ and ϕ with failure in M_z after 15s: LQR control.

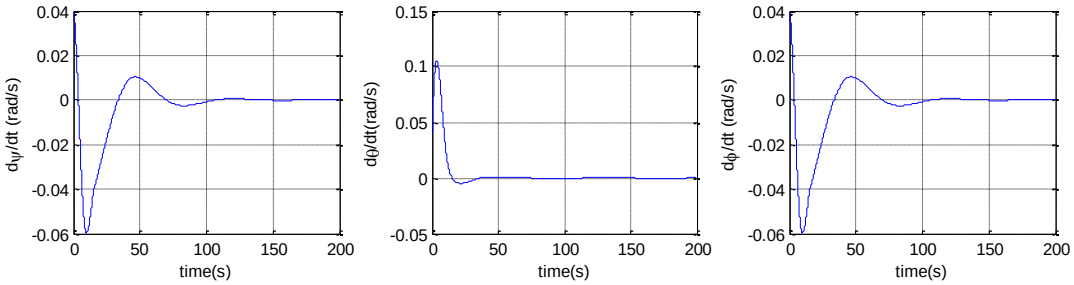

Figure 6. Angular velocity dθ/dt, dΨ/dt and dϕ/dt with the failure in M_z after 15s: LQR control.

The behaviour in this case is similar to the one when M_y fails. Even with the failure in M_z the system is stable in the other two directions. The dynamics and control in the angles θ and ϕ are able to compensate the failure in the momentum wheel acting on Ψ.

It is assumed now that the failure occurs in M_x and in M_y at the same time. The results are presented in Fig. 7 and 8.

ISSN 2176-5480

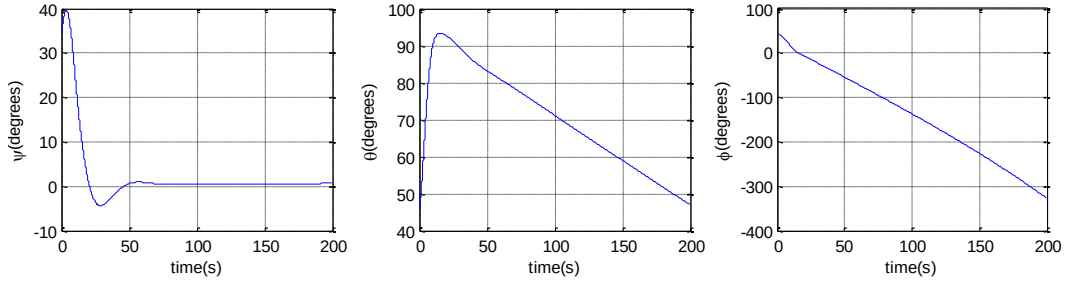

Figure 7. Attitude angles θ, Ψ and ϕ with failure in M_x and M_y after 15s: LQR control.

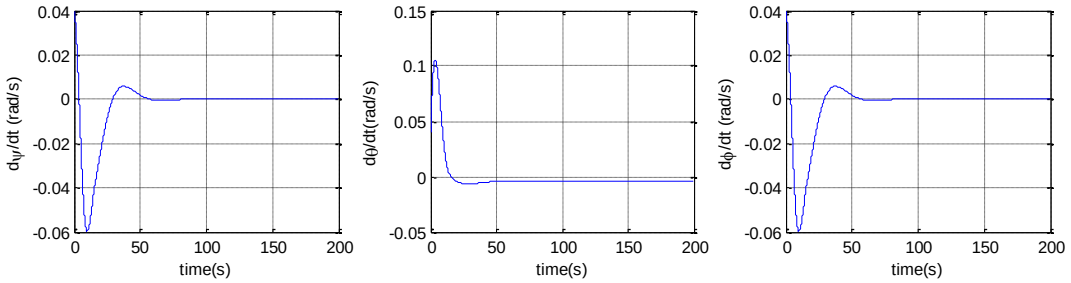

Figure 8. Angular velocity dθ/dt, dΨ/dt and dϕ/dt with the failure in M_x and M_y after 15s: LQR control.

With the simultaneous failure in the momentum wheel in the x and y directions the instability occurs in all the attitude angles. It happens because the only controlled angle, Ψ, cannot exert sufficient influence on the other two angles in order to stabilize their positions.

It is assumed now that the failure occurs in M_x and in M_z at the same time. The results are presented in Fig. 9 and 10.

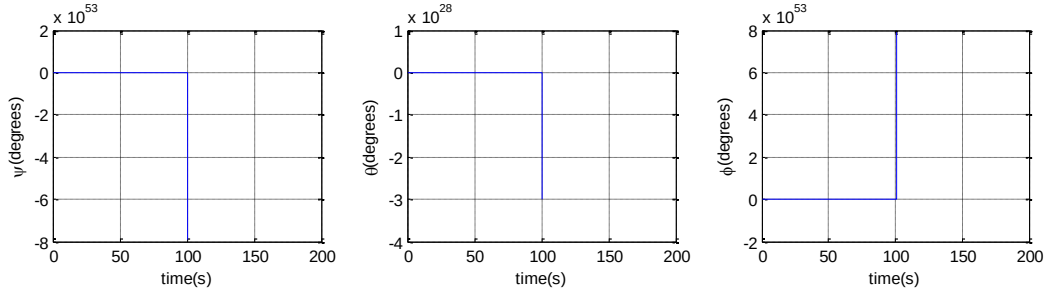

Figure 9. Attitude angles θ, Ψ and ϕ with failure in M_x and M_z after 15s: LQR control.

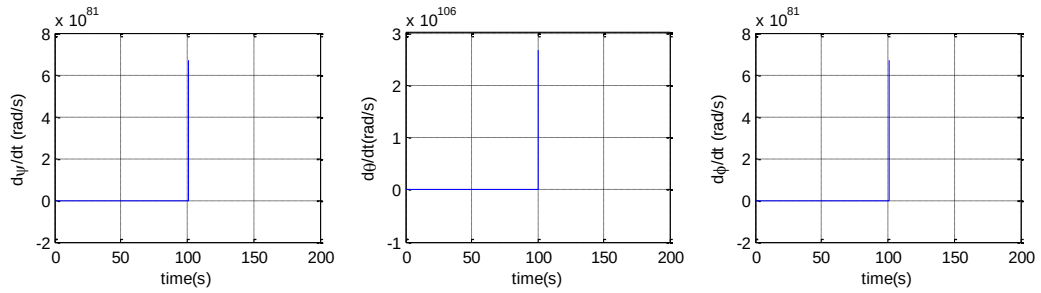

Figure 10. Angular velocity dθ/dt, dΨ/dt and dϕ/dt with the failure in M_x and M_z after 15s: LQR control.

Considering the simultaneous failure in the momentum wheels in the x and z directions the instability occurs in all the attitude angles. The coupling with the angle ϕ is not sufficient to compensate the failure in the momentum wheels related to angles θ and Ψ.

It is assumed now that the failure occurs in M_y and M_z at the same time. The results are presented in Fig. 11 and 12.

ISSN 2176-5480

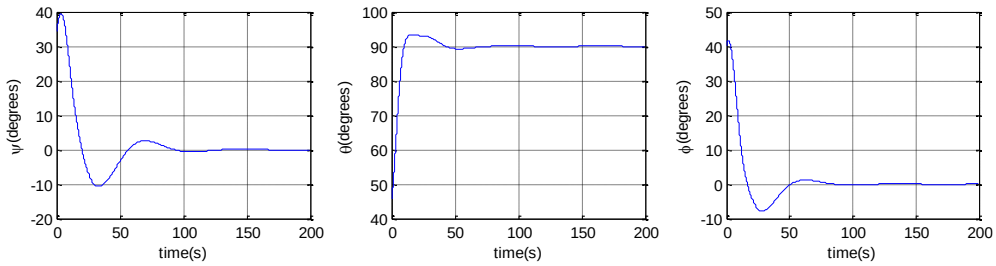

Figure 11. Attitude angles θ, Ψ and ϕ with failure in M_y and M_z after 15s: LQR control.

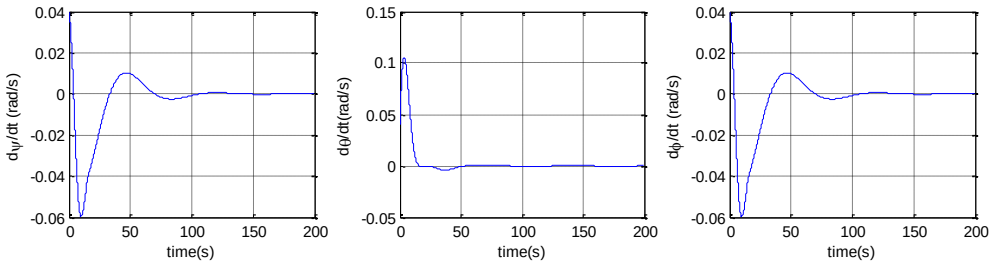

Figure 12. Angular velocity dθ/dt, dΨ/dt and dϕ/dt with the failure in M_y and M_z after 15s: LQR control.

With only the torque M_x actuating it is possible to control all the attitude angles. This is possible because of the dynamic coupling between all these angles. The momentum wheel on the x direction has influence on the angles in all the three directions. Differently from the other cases, it happens because of the relationship between the angular velocity ω in each direction and the Euler´s angles considered here.

6.2 Failure of the momentum wheel considering the SDRE

The failures on the momentum wheels are considered now using the SDRE as the control technique. The same conditions imposed before for the LQR control are considered here. The initial conditions are considered such that the nonlinear terms in the governing equation of motion are sufficiently excited.

The first case considers failure in M_x after 15 seconds of operation. The results are presented in Fig. 13 and 14.

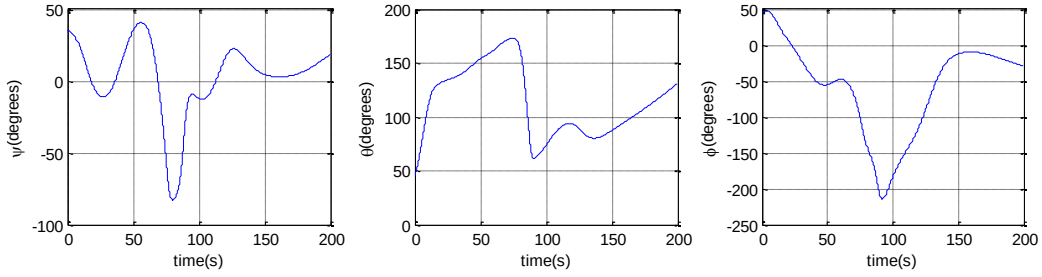

Figure 13. Attitude angles θ, Ψ and ϕ with failure in M_x after 15s: SDRE control.

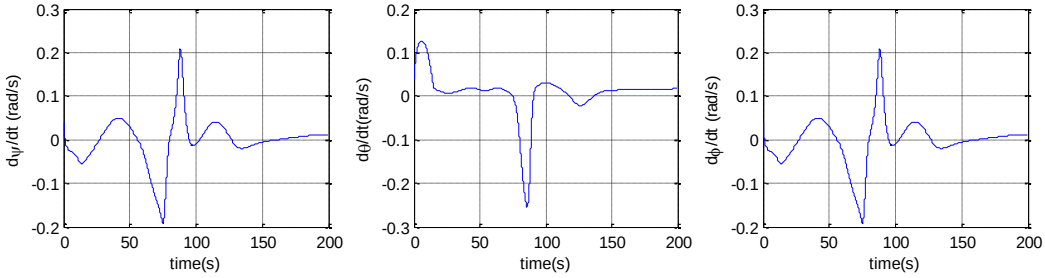

Figure 14. Angular velocity dθ/dt, dΨ/dt and dϕ/dt with the failure in M_x after 15s: SDRE control.

ISSN 2176-5480

The failure in the momentum wheel aligned with the x-axes makes the system unstable. The values of the angles and velocities are around the desired values but not converges t it.

Considering that M_y fails, the results are presented in Fig. 15 and 16.

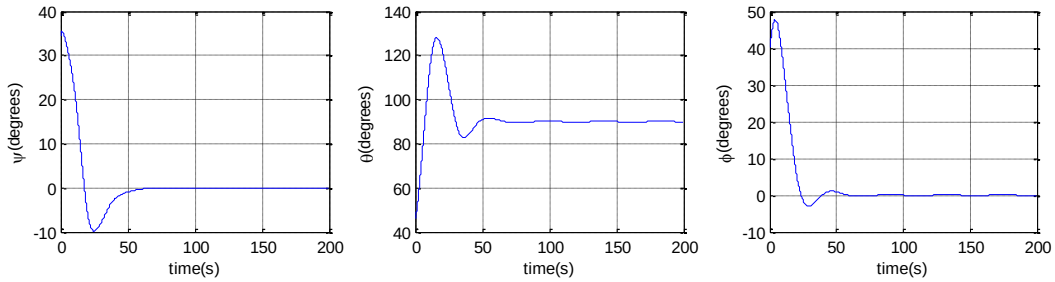

Figure 15. Attitude angles θ, Ψ and ϕ with failure in M_y after 15s: SDRE control

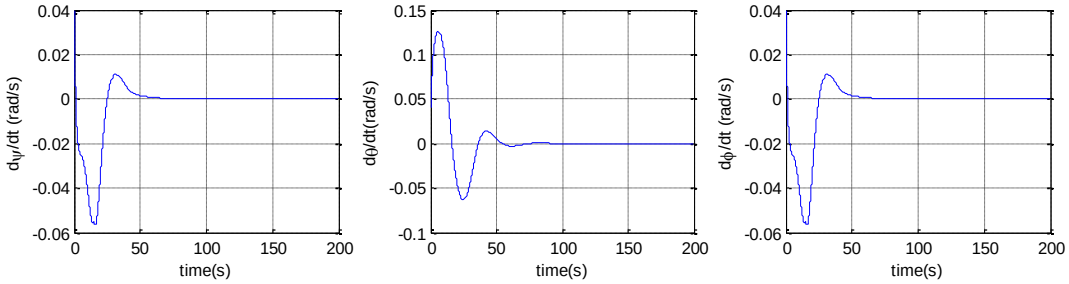

Figure 16. Angular velocity dθ/dt, dΨ/dt and dϕ/dt with the failure in M_y after 15s: SDRE control

As presented in Fig. 15 and 16, even with the failure in the momentum wheel aligned with the y-axis the system stabilizes in the desired positions. It is observed again the influence of the angular coupling between the attitude angles.

One considers now that M_z fails. The results are presented in Fig. 17 and 18.

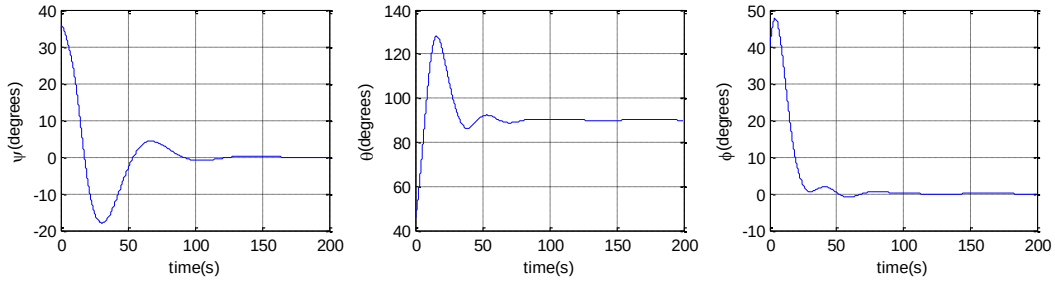

Figure 17. Attitude angles θ, Ψ and ϕ with failure in M_z after 15s: SDRE control

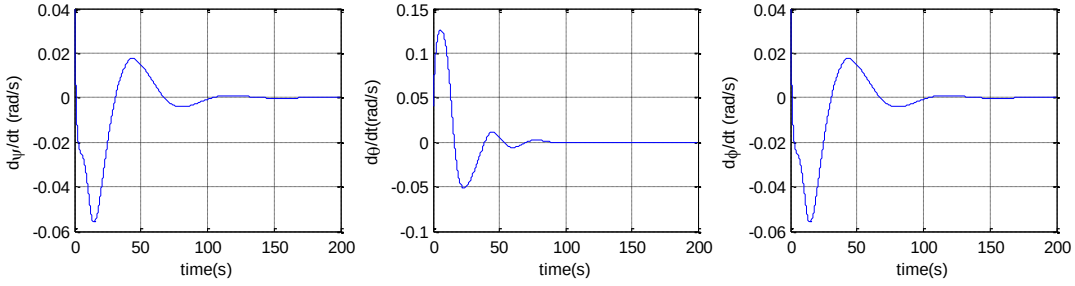

Figure 18. Angular velocity dθ/dt, dΨ/dt and dϕ/dt with the failure in M_z after 15s: SDRE control

ISSN 2176-5480

As presented in Fig. 17 and 18, with the failure in the momentum wheel aligned with the z-axes the system is stabilized in all the desired angular positions. Similar with the previous simulation, the angular coupling that θ and ϕ exert in Ψ is able to compensate the failure in the momentum wheel related to Ψ. Comparing the LQR results presented in Fig. 5 and 6 with similar results using SDRE presented in Fig. 17 and 18 the nonlinear control shows the best results.

With the failure occurring in M_x and in M_y at the same time, the results are presented in Fig. 19 and 20.

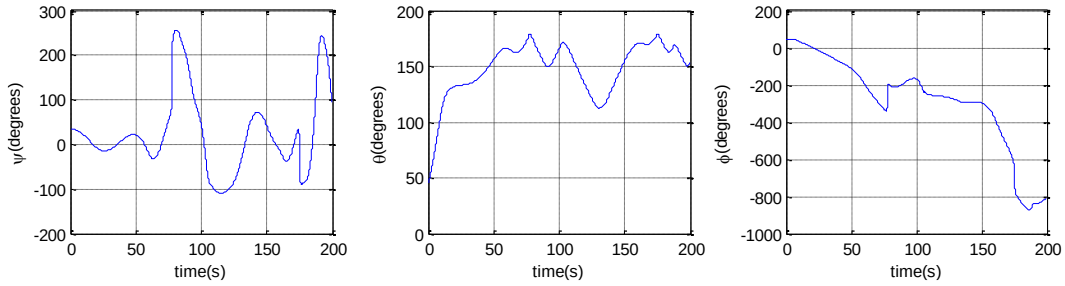

Figure 19. Attitude angles θ, Ψ and ϕ with failure in M_x and M_y after 15s: SDRE control.

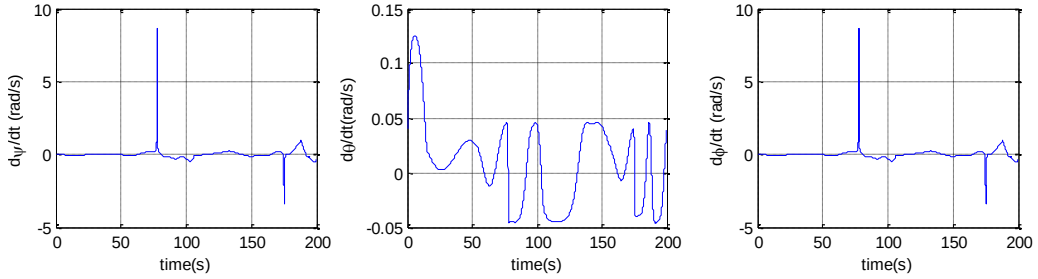

Figure 20. Angular velocity dθ/dt, dΨ/dt and dϕ/dt with the failure in M_x and M_y after 15s: SDRE control.

Considering the simultaneous failure in the momentum wheels in the x and y directions the instability occurs in all the attitude angles. This happens because Ψ cannot exert sufficient influence on the other two angles where the wheels failed in order to stabilize their positions.

Now it is assumed that the failure occurs in the x and z directions. The results are presented in Fig. 21 and 22.

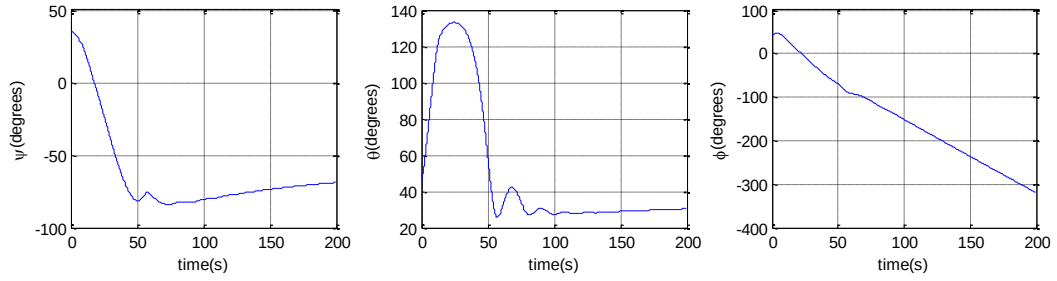

Figure 21. Attitude angles θ, Ψ and ϕ with failure in M_x and M_z after 15s: SDRE control.

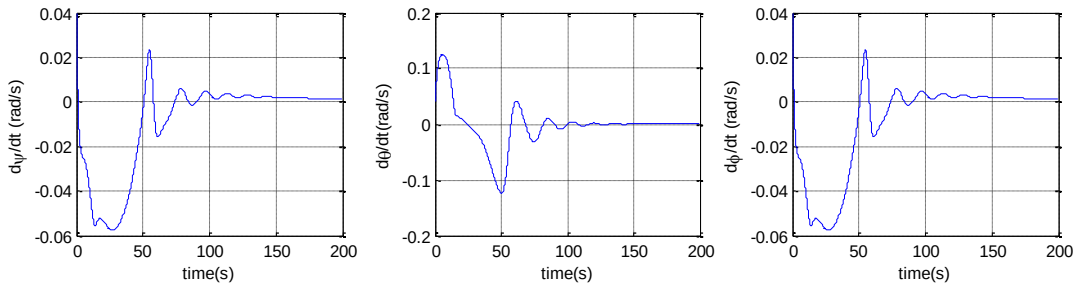

Figure 22. Angular velocity dθ/dt, dΨ/dt and dϕ/dt with the failure in M_x and M_z after 15s: SDRE control.

ISSN 2176-5480

Considering now the simultaneous failure in the momentum wheels in the x and z directions the instability also occurs in all the attitude angles. Similar to the previous results, ϕ is not able to provide sufficient influence in order to the system to be stable, since the angle of higher influence, θ, has failed. Comparing the LQR results in Fig. 9 and 10 for failure in M_x and M_z with the results for the SDRE presented in Fig. 21 and 22, one can see that the SDRE results are better.

It is assumed now failure in M_y and in M_z at the same time. The results are presented in Fig. 23 and 24.

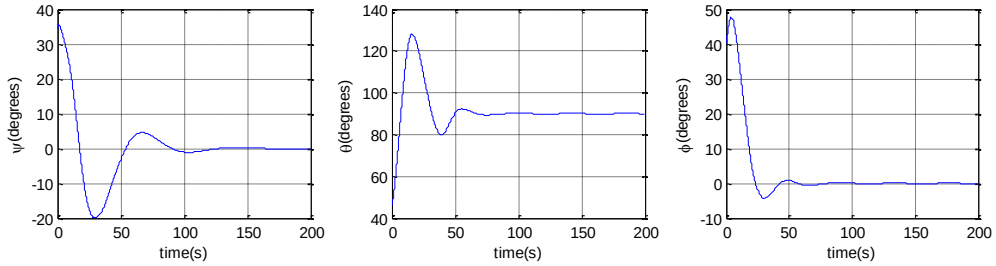

Figure 23. Attitude angles θ, Ψ and ϕ with failure in M_y and M_z after 15s: SDRE control

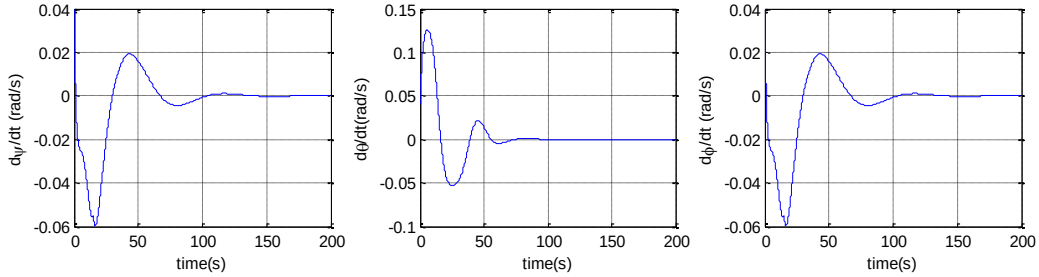

Figure 24. Angular velocity $d\theta/dt$, $d\Psi/dt$ and $d\phi/dt$ with the failure in M_y and M_z after 15s: SDRE control

Considering only the torque M_x actuating it is possible to control all the attitude angles as occurs when applying the LQR control. This is possible because the stronger dynamic coupling between all the attitude angles. The momentum wheel on the x direction has strong influence on the angles in all the three directions.

7. CONCLUSION

The governing equations of motion for the satellite are a nonlinear set. Because of its nonlinear nature, the variables are coupled and a change in any of them (θ, ϕ or ψ and its derivatives) involves a change in the other two variables. This coupling also occurs with the torque controls. The actuator considered here are the momentum wheels.

In this paper is considered failures in the momentum wheel in several situations. In some cases only one actuator fails and in some cases two actuators fails.

It is possible to conclude that the system can only be satisfactorily controlled if the momentum wheel in the x direction of the x (related to the angle θ) does not fail, regardless what happens with the other two momentum wheels. This fact can be explained by the coupling between the variables of the problem and also by the transformation of the Euler angles chosen in the mathematical model of the system.

In many situations it is clear that the nonlinear control SDRE presents better results when compared with the linear control LQR.

8. REFERENCES

Agrawal , B. N., “Design of Geosynchronous Spacecraft”, Prentice Hall, University of Michigan. 1986.

Fenili, A. e Kuga, H. K., “Controle de altitude de satélites rígido-flexíveis usando a otimização extrema generalizada com abordagem multi-objetivo” Instituto Nacional de Pesquisas Espaciais (INPE), Technical Report. 2008.

Çimen, T., “State-Dependent Riccati Equation (SDRE): A Survey”, Proceedings of the 17th World Congress, The International Federation of Automatic Control, Seoul, Korea, July 6-11, pp 3761-3775,2008.

Dorato, P., Abdallah, C., Cerone, V., “Linear-Quadratic Control – An Introduction”, Prentice Hall, Englewood Cliffs, New Jersey, 1995.

Shamma, J. S., Cloutier, J. R., “Existence of SDRE Stabilizing Feedback”, IEEE Transactions on Automatic Control, 48, 513-517, 2003.